INSTITUTE OF PHYSICS PUBLISHING JOURNAL OF PHYSICS B: ATOMIC, MOLECULAR AND OPTICAL PHYSICS

J. Phys. B: At. Mol. Opt. Phys. **39** (2006) 4239–4247 doi:10.1088/0953-4075/39/20/021

Hyperfine induced interference effects in the 4s4d $^3D_2$–4s4f $^3F_{2,3}$ transitions in Ga II

Martin Andersson[1], **Per Jönsson**[1,2] **and Hans Sabel**[3]

[1] Department of Physics, Lund University, Box 118, S-221 00 Lund, Sweden
[2] Teachers Education, Malmö University, S-205 06 Malmö, Sweden
[3] Atomic Astrophysics, Lund Observatory, Lund University, Box 43, S-221 00 Lund, Sweden

E-mail: martin.andersson@fysik.lu.se

Received 13 July 2006, in final form 25 August 2006
Published 10 October 2006
Online at stacks.iop.org/JPhysB/39/4239

Abstract

We report relativistic multiconfiguration Dirac–Hartree–Fock calculations of transitions between the hyperfine levels of 4s4f $^3F_{2,3}$ and 4s4d $^3D_2$ in Ga II. The capacity of two newly developed programs connected to the graspVU package for generating synthetic spectra is explored. The obtained theoretical spectra are compared to Fourier transform spectra and good agreement is found. The importance of hyperfine induced interference effects for the 4s4d $^3D_2$–4s4f $^3F_2$ transitions is pointed out, and the gf values for all the hyperfine transitions are given.

1. Introduction

In high resolution stellar spectra many lines are broadened due to unresolved or partly resolved hyperfine and isotope structures. For magnetic stars the complexity increases even further due to the splitting of the fine and hyperfine levels. To aid the analyses of these spectra, two new programs, HFSZEEMAN [1] and MTRANS [2], have been developed. Based on multiconfiguration Dirac–Hartree–Fock wavefunctions from the graspVU package [3], the first program computes relevant hyperfine and Zeeman matrix elements and constructs the total interaction matrix for an atom in an external magnetic field. By diagonalizing the interaction matrix the splittings of fine and hyperfine levels are obtained for the given values of the magnetic field. From calculated transition rates the second program determines the distribution of the transition strength among the different lines between magnetic sublevels. Finally, adding Doppler profiles to each component, synthetic spectra are generated.

In this paper the HFSZEEMAN and MTRANS programs are used in the field free limit to generate spectra for the 4s4d $^3D_2$–4s4f $^3F_{2,3}$ transitions in Ga II. Gallium has two stable isotopes with the natural composition of 60% ^{69}Ga and 40% ^{71}Ga, both with nuclear spin $I = 3/2$. The nuclear magnetic moments are, respectively, $2.01659\mu_N$ and $2.56227\mu_N$. The transitions, which were recently recorded with Fourier transform spectroscopy, exhibit wide, partly resolved patterns.

Due to small fine structure and term splittings of 4s4f, off-diagonal hyperfine interactions become important leading to line positions and intensity distributions that cannot be explained using the normal assumptions of the spectral analysis [4]. The studied lines are unblended and potentially important for the ongoing abundance analysis in chemically peculiar HgMn stars, where gallium is overabundant. In recent studies the abundance differs for studies in the optical region [5, 6] and the UV region [7, 8]. Dworetsky *et al* [9] referred to this as 'the gallium problem', and explained the discordant results by the need for a hyperfine structure of spectral lines located in the optical region. Karlsson and Litzen [4] studied the hyperfine and isotope structure of 18 Ga II lines, recorded with Fourier transform spectroscopy, which all were important lines for the abundance analysis, but only 12 of these could be analysed. A study based on these results [10] could still not explain the differences. Lack of accurate oscillator strengths was pointed out [10]. This was re-emphasized [11] and the warrant for more accurate line structures was also pointed out.

2. Theory

2.1. Hyperfine interaction

The hyperfine structure of an atomic level is caused by the non-central interaction between the electrons and the electromagnetic multipole moments of the nucleus. The Hamiltonian for the interaction is often given as

$$H_{\rm hfs} = \mathbf{T}^{(1)} \cdot \mathbf{M}^{(1)} + \mathbf{T}^{(2)} \cdot \mathbf{M}^{(2)}, \tag{1}$$

where $\mathbf{T}^{(k)}$ and $\mathbf{M}^{(k)}$ are spherical tensor operators of rank k in the electronic and nuclear spaces, respectively. The $k = 1$ term represents the magnetic dipole interaction and the $k = 2$ term the electric quadrupole interaction. Explicit expressions for the electronic tensor operators can be found in the write up of the relativistic hyperfine structure program belonging to graspVU [12]. The hyperfine interaction couples the nuclear I and electronic J angular momenta to a total momentum $F = I + J$. Denoting the nuclear and electronic wavefunctions by $|IM_I\rangle$ and $|\gamma JM_J\rangle$, respectively, the zero-order wavefunctions of the coupled states can be written as

$$|\gamma IJFM_F\rangle = \sum_{M_I, M_J} \langle IJM_IM_J|IJFM_F\rangle |IM_I\rangle|\gamma JM_J\rangle. \tag{2}$$

If the hyperfine interaction is weak so that the interaction energy is small compared to the fine-structure separation, $H_{\rm hfs}$ can be treated in the first-order perturbation theory. A fine-structure level γJ is then split according to

$$\langle \gamma IJFM_F|\mathbf{T}^{(1)} \cdot \mathbf{M}^{(1)} + \mathbf{T}^{(2)} \cdot \mathbf{M}^{(2)}|\gamma IJFM_F\rangle. \tag{3}$$

We express this in terms of the reduced electronic and nuclear matrix elements,

$$\langle \gamma IJFM_F|\mathbf{T}^{(1)} \cdot \mathbf{M}^{(1)}|\gamma IJFM_F\rangle = (-1)^{I+J+F} \begin{Bmatrix} I & J & F \\ J & I & 1 \end{Bmatrix} \times \sqrt{2J+1}\sqrt{2I+1}\langle \gamma J\|\mathbf{T}^{(1)}\|\gamma J\rangle\langle I\|\mathbf{M}^{(1)}\|I\rangle, \tag{4}$$

$$\langle \gamma IJFM_F|\mathbf{T}^{(2)} \cdot \mathbf{M}^{(2)}|\gamma IJFM_F\rangle = (-1)^{I+J+F} \begin{Bmatrix} I & J & F \\ J & I & 2 \end{Bmatrix} \times \sqrt{2J+1}\sqrt{2I+1}\langle \gamma J\|\mathbf{T}^{(2)}\|\gamma J\rangle\langle I\|\mathbf{M}^{(2)}\|I\rangle. \tag{5}$$

Factorizing the dependence on the F quantum number and using the relations

$$\langle I\|\mathbf{M}^{(1)}\|I\rangle = \mu_I\sqrt{\frac{(I+1)}{I}}, \tag{6}$$

$$\langle I\|\mathbf{M}^{(2)}\|I\rangle = \frac{Q}{2}\sqrt{\frac{(2I+3)(I+1)}{I(2I-1)}}, \tag{7}$$

the energies can be expressed in terms of the hyperfine interaction constants

$$A_J = \frac{\mu_I}{I}\frac{1}{\sqrt{J(J+1)}}\langle\gamma J\|\mathbf{T}^{(1)}\|\gamma J\rangle, \tag{8}$$

$$B_J = 2Q\sqrt{\frac{J(2J-1)}{(J+1)(2J+3)}}\langle\gamma J\|\mathbf{T}^{(2)}\|\gamma J\rangle, \tag{9}$$

and we have

$$\Delta E = \frac{1}{2}A_J C + B_J\frac{\frac{3}{4}C(C+1) - I(I+1)J(J+1)}{2I(2I-1)J(2J-1)}, \tag{10}$$

where $C = F(F+1) - J(J+1) - I(I+1)$.

To account for off-diagonal hyperfine effects we consider the total Hamiltonian

$$H = H_{\mathrm{DCB}} + H_{\mathrm{hfs}}. \tag{11}$$

Now only F and M_F are good quantum numbers and we represent the wavefunction by an expansion

$$|\gamma F M_F\rangle = \sum_{\alpha J} c_{\alpha J}|\alpha I J F M_F\rangle. \tag{12}$$

This leads to the matrix eigenvalue problem $\mathbf{Hd} = E\mathbf{c}$, where $\mathbf{H}$ is the matrix with elements

$$H_{\alpha I J F,\alpha' I J' F} = \langle\alpha I J F M_F|H_{\mathrm{DCB}} + H_{\mathrm{hfs}}|\alpha' I J' F M_F\rangle. \tag{13}$$

The matrix elements of the Dirac–Coulomb–Breit Hamiltonian H_{DCB} are diagonal in all quantum numbers and equal the Dirac–Coulomb–Breit Hamiltonian eigenvalues. The hyperfine interaction matrix elements can be expressed in terms of reduced electronic and nuclear matrix elements. The relevant matrix elements are

$$\langle\gamma I J F M_F|\mathbf{T}^{(1)}\cdot\mathbf{M}^{(1)}|\gamma' I J' F M_F\rangle = (-1)^{I+J+F}\begin{Bmatrix} I & J & F \\ J' & I & 1 \end{Bmatrix} \times\sqrt{2J+1}\sqrt{2I+1}\langle\gamma J\|\mathbf{T}^{(1)}\|\gamma' J'\rangle\langle I\|\mathbf{M}^{(1)}\|I\rangle, \tag{14}$$

where $J' = J-1, J$ and

$$\langle\gamma I J F M_F|\mathbf{T}^{(2)}\cdot\mathbf{M}^{(2)}|\gamma' I J' F M_F\rangle = (-1)^{I+J+F}\begin{Bmatrix} I & J & F \\ J' & I & 2 \end{Bmatrix} \times\sqrt{2J+1}\sqrt{2I+1}\langle\gamma J\|\mathbf{T}^{(2)}\|\gamma' J'\rangle\langle I\|\mathbf{M}^{(2)}\|I\rangle, \tag{15}$$

where $J' = J-2, J-1, J$.

2.2. Transition probabilities

When the off-diagonal hyperfine interaction is weak the oscillator strengths of the hyperfine components for an electric dipole transition are given in terms of the zero-order wavefunctions of the upper and lower fine-structure levels,

$$\begin{aligned}\mathrm{gf}(\gamma I J F - \gamma' I J' F') &= \frac{2}{3}\Delta E |\langle \gamma I J F \| \mathbf{P}^{(1)} \| \gamma I J' F' \rangle|^2 \\ &= \frac{2}{3}\Delta E (2F+1)(2F'+1) \begin{Bmatrix} J & I & F \\ F' & 1 & J' \end{Bmatrix}^2 |\langle \gamma J \| \mathbf{P}^{(1)} \| \gamma' J' \rangle|^2. \end{aligned} \tag{16}$$

From the above expression we see that the relative strengths of the various lines of the hyperfine multiplet are governed by the square of a 6-j symbol. In the general case, where off-diagonal hyperfine interaction is included, the oscillator strengths are given by

$$\begin{aligned}\mathrm{gf}(\gamma F - \gamma' F') &= \frac{2}{3}\Delta E \left| \sum_{\alpha J} \sum_{\alpha' J'} c_{\alpha J} c_{\alpha' J'} \langle \alpha I J F \| \mathbf{P}^{(1)} \| \alpha' I J' F' \rangle \right|^2 \\ &= \frac{2}{3}\Delta E (2F+1)(2F'+1) \left| \sum_{\alpha J} \sum_{\alpha' J'} c_{\alpha J} c_{\alpha' J'} \begin{Bmatrix} J & I & F \\ F' & 1 & J' \end{Bmatrix} \langle \alpha J \| \mathbf{P}^{(1)} \| \alpha' J' \rangle \right|^2. \end{aligned} \tag{17}$$

If the different terms of the summation are of the same size there are interference effects leading to large redistributions of oscillator strengths.

2.3. Synthetic spectrum

From the calculated transition energies and oscillator strengths a synthetic spectrum can be generated for the transition array. Following [4], it is assumed that each hyperfine component has a Gaussian–Doppler profile with a given full width half maximum (FWHM). If there are more than one isotope in the atomic sample the widths of the different isotopic components should be scaled according to the inverse of the square roots of the isotope masses. The intensity for the hyperfine components within an isotope is distributed according to the expressions for the gf values above. The intensity ratios between the hyperfine components of the isotopes are scaled according to the abundance of the isotopes.

3. Atomic data

As a test case of the HFSZEEMAN and MTRANS programs we look at the spectra for the 4s4d $^3D_2$–4s4f $^3F_{2,3}$ transitions in Ga II. Gallium has two stable isotopes with the natural composition of 60% ^{69}Ga and 40% ^{71}Ga, both with nuclear spin $I = 3/2$ leading to a transition array where the F quantum numbers of the upper 4s4f $^3F_{2,3}$ states go between $7/2$ and $1/2$, and $9/2$ and $3/2$, respectively. The F quantum numbers for the 4s4d $^3D_2$ state lie between $7/2$ and $1/2$.

We represent the wavefunctions for the hyperfine levels of 4s4f $^3F_{2,3}$ using coupled electronic and nuclear functions, where the electronic part consists of all fine-structure levels of the 4s4f configuration. In a similar way the wavefunctions for the hyperfine levels of 4s4d $^3D_2$ are constructed using electronic functions belonging to the fine-structure levels of 4s4d. The electronic wavefunctions for the fine-structure levels of the 4s4f and 4s4d configurations were taken from the previous multiconfiguration Dirac–Hartree–Fock (MCDHF) calculations by the present authors [13]. The configuration expansions for the levels were obtained using the active set method, where the active sets were increased in a systematic way by adding five

Table 1. Calculated fine structure and term splitting of 4s4d and 4s4f in cm^{-1} compared with experimental values.

	$^3D_1$	$^3D_2$	$^3D_3$	$^1D_2$
DF	0	23.63	59.96	21 756.12
RCI	0	24.99	63.72	12 849.03
Exp.[a]	0	26.27	67.27	12 371.55
	$^3F_2$	$^3F_3$	$^3F_4$	$^1F_3$
DF	0	−0.08	−0.19	139.09
RCI	0	0.43	6.71	9.24
Exp.[a]	0	0.98	7.29	10.09

[a] Isberg and Litzén [16].

Table 2. Calculated oscillator strengths in Coulomb (velocity) and Babushkin (length) gauges and transition energies in cm^{-1} for transitions between the fine-structure levels of 4s4d and 4s4f.

ΔE^{a}_{exp}	ΔE_{calc}	Transition	gf_C	gf_B
23 516	23 488	4s4d $^3D_1$–4s4f $^3F_2$	2.64 [0]	2.65 [0]
23 490	23 463	4s4d $^3D_2$–4s4f $^3F_2$	4.88 [−1]	4.91 [−1]
23 490	23 464	4s4d $^3D_2$–4s4f $^3F_3$	2.82 [0]	2.83 [0]
23 500	23 472	4s4d $^3D_2$–4s4f $^1F_3$	1.10 [0]	1.10 [0]
23 449	23 425	4s4d $^3D_3$–4s4f $^3F_2$	1.40 [−2]	1.40 [−2]
23 450	23 425	4s4d $^3D_3$–4s4f $^3F_3$	3.53 [−1]	3.55 [−1]
23 459	23 434	4s4d $^3D_3$–4s4f $^1F_3$	1.36 [−1]	1.36 [−1]
23 457	23 431	4s4d $^3D_3$–4s4f $^3F_4$	5.69 [0]	5.70 [0]
11 145	10 639	4s4d $^1D_2$–4s4f $^3F_2$	4.73 [−6]	3.90 [−6]
11 146	10 640	4s4d $^1D_2$–4s4f $^3F_3$	8.39 [−1]	6.29 [−1]
11 155	10 648	4s4d $^1D_2$–4s4f $^1F_3$	2.16 [0]	1.62 [0]

[a] Karlsson and Litzén [4].

layers of correlation orbitals. Core–valence correlation was accounted for by allowing single excitations from the 3d core-shell. Spin and orbital polarization, which are of importance for the hyperfine structure constants [14], were included in the final relativistic configuration interaction (RCI) calculations by adding configuration state functions generated by single excitations from all core shells. In the RCI calculation the Breit interaction [15] and leading QED corrections were also included.

The fine-structure and term separations are of crucial importance in the calculations of the off-diagonal effects and in table 1 the calculated separations are compared with experimental values by Isberg and Litzén [16]. The energy splittings in the final RCI calculation are in good agreement with experiment; this is particularly true for the 4s4f splittings that are off by very large quantities at the Dirac–Fock (DF) level. Weighted oscillator strengths between the fine-structure levels of the two configurations are displayed in table 2. The reduced matrix elements of the magnetic dipole and electric quadrupole hyperfine operators between the fine-structure levels of 4s4d and 4s4f are shown in table 3. Based on the good agreement between theory and experiment for other hyperfine interaction constants in Ga II [13] we believe that the matrix elements are accurate to within a few percent.

4. Generation of spectra

Using the experimental fine-structure energies in table 1, the reduced hyperfine interaction matrix elements in table 3 and values of the nuclear magnetic dipole μ_I and quadrupole

Table 3. Reduced magnetic dipole $\langle \gamma J \| \mathbf{T}^{(1)} \| \gamma' J' \rangle$ and electric quadrupole $\langle \gamma J \| \mathbf{T}^{(2)} \| \gamma' J' \rangle$ interaction matrix elements between the fine-structure levels of 4s4d and 4s4f.

	$^3D_3$	$^3D_2$	$^1D_2$	$^3D_1$
	Reduced magnetic dipole matrix elements			
$^3D_3$	4.2383 [−1]	−2.9503 [−1]	−2.4455 [−1]	0.0000 [0]
$^3D_2$	−2.9503 [−1]	1.5549 [−1]	−2.4471 [−1]	3.4419 [−1]
$^1D_2$	−2.4455 [−1]	−2.4471 [−1]	4.3328 [−2]	−1.8655 [−1]
$^3D_1$	0.0000 [0]	3.4419 [−1]	−1.8655 [−1]	−2.5193 [−1]
	Reduced electric quadrupole matrix elements			
$^3D_3$	1.7741 [−1]	1.1853 [−1]	6.5428 [−3]	−3.9514 [−2]
$^3D_2$	1.1853 [−1]	1.0023 [−1]	−1.7609 [−2]	−1.2689 [−1]
$^1D_2$	6.5428 [−3]	−1.7609 [−2]	2.1367 [0]	5.0930 [−3]
$^3D_1$	−3.9514 [−2]	−1.2689 [−1]	5.0930 [−3]	1.1981 [−1]

	$^3F_4$	$^3F_3$	$^1F_3$	$^3F_2$
	Reduced magnetic dipole matrix elements			
$^3F_3$	4.2234 [−1]	4.7650 [−1]	1.4881 [−1]	0.0000 [0]
$^3F_2$	4.7650 [−1]	−2.5837 [−1]	−2.1695 [−1]	−1.4520 [−1]
$^1F_2$	1.4881 [−1]	−2.1695 [−1]	3.6832 [−1]	4.6501 [−1]
$^3F_1$	0.0000 [0]	−1.4520 [−1]	4.6501 [−1]	−3.0757 [−1]
	Reduced electric quadrupole matrix elements			
$^3F_4$	2.7897 [−2]	−1.1609 [−2]	6.6800 [−3]	−2.9478 [−3]
$^3F_3$	−1.1609 [−2]	2.6482 [−2]	4.5144 [−3]	1.2614 [−2]
$^1F_3$	6.6800 [−3]	4.5144 [−3]	2.9961 [−2]	8.1702 [−3]
$^3F_1$	−2.9478 [−3]	1.2614 [−2]	−8.1702 [−3]	2.6480 [−2]

moments Q of the two isotopes the HFSZEEMAN program constructs and diagonalizes the Hamiltonian for each of the possible F symmetries connected with, respectively, 4s4d $^3D_2$ and 4s4f $^3F_{2,3}$ to yield energies $E_{\gamma F}$ and wavefunctions expansions

$$|\gamma F M_F\rangle = \sum_{\alpha J} c_{\alpha J} |\alpha I J F M_F\rangle. \tag{18}$$

From the above wavefunction expansions and the transition data in table 2 the oscillator strengths between the different hyperfine levels of 4s4d $^3D_2$ and 4s4f $^3F_{2,3}$ are evaluated by the MTRANS program. The results are displayed in tables 4 and 5. To see the importance of the off-diagonal hyperfine interaction, weighted oscillator strengths resulting from equation (16) are also displayed. For 4s4d $^3D_2$–4s4f $^3F_2$ the effects of the off-diagonal hyperfine interaction are quite large and it is obvious that they need to be included in a rigorous way.

Using a Matlab utility program accompanying the MTRANS program a synthetic spectrum was generated for the transition arrays. In the spectrum each hyperfine component in ^{69}Ga has a Gaussian–Doppler profile with a given FWHM. The Doppler width for ^{71}Ga was scaled compared with ^{69}Ga with a factor 0.986 which is the ratio of the inverse of the square roots of the masses of the two isotopes. The intensity of the hyperfine components within each isotope was distributed according to the values in tables 4 and 5, and weighted in accordance to the relative abundance of the two isotopes. Finally, the transition arrays for the two isotopes were displaced to account for the isotope shift. Some testing showed that the Doppler profiles for ^{69}Ga with FWHM = 7.5×10^{-2} cm^{-1}, an isotopic shift of 6×10^{-3} cm^{-1} and a displacement of the whole synthetic spectra by 27.47 cm^{-1} gave a very good agreement with experiment. The generated synthetic spectra are displayed in figure 1 together with the Fourier transform

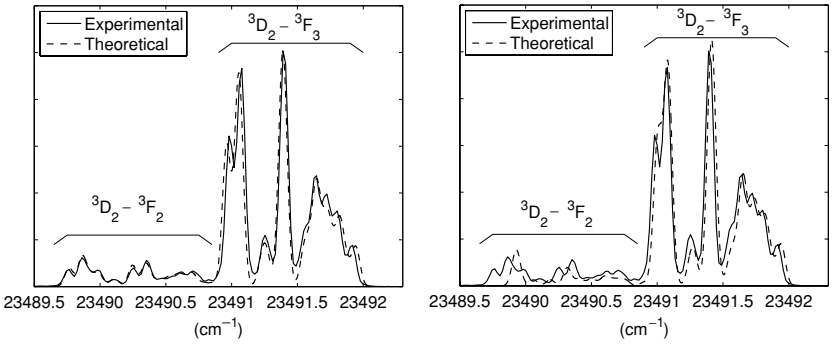

Figure 1. Comparison of theoretical and experimental spectra for the transitions between 4s4d $^3D_2$ and 4s4f $^3F_{2,3}$. The figure on the left displays the spectra where the off-diagonal hyperfine interaction has been included. The figure on the right displays the spectra generated using only the diagonal part of the hyperfine interaction.

Table 4. Transition energies relative the strongest transition in the spectrum in cm^{-1} and weighted oscillator strengths in the Babushkin (length) gauge for all hyperfine transitions between 4s4d $^3D_2$ and 4s4f $^3F_2$ in ^{69}Ga and ^{71}Ga. The weighted oscillator strengths for pure coupling are from calculations omitting all off-diagonal hyperfine interaction matrix elements.

		^{69}Ga		^{71}Ga		Pure coupling
$F_{^3D_2}$	$F_{^3F_2}$	ΔE^a	gf_B	ΔE^a	gf_B	gf_B
7/2	7/2	0	5.46 [−1]	−0.105	5.18 [−1]	6.74 [−1]
5/2	7/2	0.126	2.49 [−1]	0.054	2.85 [−1]	1.12 [−1]
7/2	5/2	0.257	9.84 [−2]	0.220	9.47 [−2]	1.12 [−1]
5/2	5/2	0.383	2.47 [−1]	0.378	2.25 [−1]	3.40 [−1]
3/2	5/2	0.476	2.70 [−1]	0.497	3.09 [−1]	1.38 [−1]
5/2	3/2	0.580	1.27 [−1]	0.633	1.24 [−1]	1.38 [−1]
3/2	3/2	0.673	1.18 [−1]	0.752	1.07 [−1]	1.57 [−1]
1/2	3/2	0.731	1.67 [−1]	0.825	1.89 [−1]	9.83 [−2]
3/2	1/2	0.799	1.01 [−1]	0.917	1.02 [−1]	9.83 [−2]
1/2	1/2	0.586	1.02 [−1]	0.991	1.03 [−1]	9.83 [−2]

[a] Energies relative the strongest transition at 23 489.664 cm^{-1}.

Table 5. Transition energies relative the strongest transition in the spectrum in cm^{-1} and weighted oscillator strengths in the Babushkin (length) gauge for all hyperfine transitions between 4s4d $^3D_2$ and 4s4f $^3F_3$ in ^{69}Ga and ^{71}Ga. The weighted oscillator strengths for pure coupling are from the calculations omitting all off-diagonal hyperfine interaction matrix elements.

		^{69}Ga		^{71}Ga		Pure coupling
$F_{^3D_2}$	$F_{^3F_3}$	ΔE^a	gf_B	ΔE^a	gf_B	gf_B
7/2	9/2	0	3.95 [0]	−0.099	3.92 [0]	4.05 [0]
7/2	7/2	0.209	5.55 [−1]	0.168	5.73 [−1]	4.63 [−1]
5/2	7/2	0.335	2.64 [0]	0.327	2.60 [0]	2.78 [0]
7/2	5/2	0.373	3.38 [−2]	0.381	3.65 [−2]	2.32 [−2]
5/2	5/2	0.499	6.82 [−1]	0.539	7.02 [−1]	5.93 [−1]
3/2	5/2	0.592	1.72 [0]	0.658	1.69 [0]	1.82 [0]
5/2	3/2	0.615	4.40 [−2]	0.691	4.74 [−2]	3.24 [−2]
3/2	3/2	0.708	5.06 [−1]	0.809	5.19 [−1]	4.54 [−1]
1/2	3/2	0.766	1.11 [0]	0.882	1.10 [0]	1.13 [0]

[a] Energies relative the strongest transition at 23 490.855 cm^{-1}.

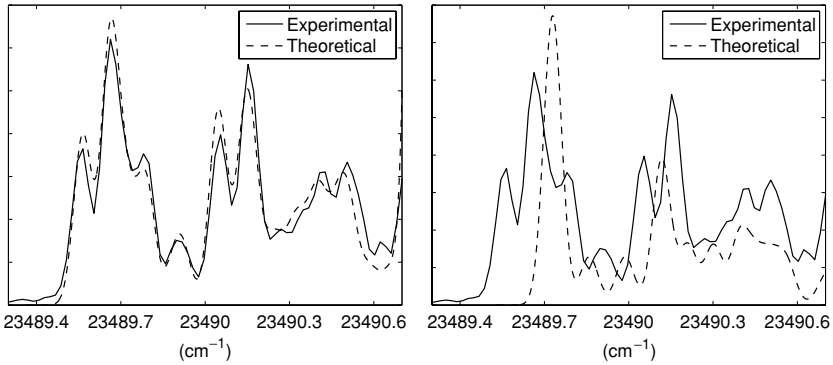

Figure 2. Comparison of theoretical and experimental spectra for the transitions between 4s4d $^3D_2$ and 4s4f $^3F_2$. The figure on the left displays the spectra where the off-diagonal hyperfine interaction has been included. The figure on the right displays the spectra generated using only the diagonal part of the hyperfine interaction.

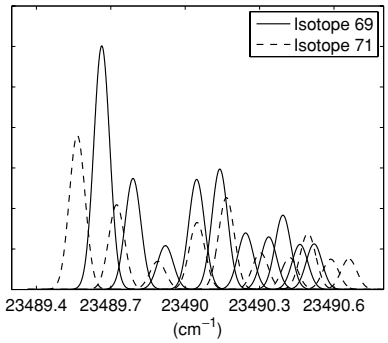

Figure 3. Spectra of the individual lines in the synthetic spectrum. Solid and dashed lines show, respectively, the contributions from ^{69}Ga and ^{71}Ga.

spectra. For comparison the synthetic spectra based on the weighted oscillator strengths from equation (16) are shown on the right. Closeups of the parts belonging to 4s4d $^3D_2$–4s4f $^3F_2$ are depicted in figure 2. From this figure the dramatic effects of the redistribution of oscillator strengths due to the hyperfine induced interference terms in equation (17) are clearly seen. The individual hyperfine components building the synthetic spectrum are shown in figure 3.

5. Summary and conclusions

We report on hyperfine interference effects in the 4s4d $^3D_2$–4s4f $^3F_{2,3}$ transitions in Ga II. From calculated electronic hyperfine and transition matrix elements synthetic spectra are generated that are compared with the previous Fourier transform spectra. The agreement between the two spectra is very good and the theoretical data could serve as starting values for the nonlinear least-squares fit to the experimental spectrum.

We have shown that the hyperfine interaction redistributes the intensity among the hyperfine transitions and theoretical relative position and weighted oscillator strengths for all hyperfine transitions 4s4d $^3D_2$–4s4f $^3F_{2,3}$ are reported. To our knowledge this has never been reported before and this could be of interest in the ongoing studies of the Ga abundance analysis of peculiar HgMn stars.

Acknowledgment

This work was supported by the Swedish Research Council (Vetenskapsrådet).

References

[1] Andersson M and Jönsson P 2006 *Comput. Phys. Commun.* submitted, the program is available from the authors upon request
[2] Andersson M and Jönsson P 2006 in preparation, the program is available from the authors upon request
[3] Jönsson P, He X and Froese Fischer C 2006 *Comput. Phys. Commun.* submitted, the graspVU source code and the corresponding manual can be downloaded from http://atoms.vuse.vanderbilt.edu/Elements/CompMeth/graspVU_0229.tar.gz
[4] Karlsson H and Litzén U 2000 *J. Phys. B: At. Mol. Opt. Phys.* **33** 2929
[5] Adelman S-J 1989 *Mon. Not. R. Astron. Soc.* **239** 487
[6] Lanz T, Artru M C, Didelon P and Mathys G 1993 *Astron. Astrophys.* **272** 465
[7] Takada-Hidai M, Sadakane K and Jugaku J 1986 *Astrophys. J.* **304** 425
[8] Smith K-C 1996 *Astron. Astrophys.* **305** 902
[9] Dworetsky M-M, Jomaron C-M and Smith C-A 1998 *Astron. Astrophys.* **333** 665
[10] Nielsen K, Karlsson H and Wahlgren G-M 2000 *Astron. Astrophys.* **363** 815
[11] Nielsen K, Wahlgren G-M, Proffitt C-R, Lecrone D-S and Adelman S-J 2005 *Astrophys. J.* **130** 2312
[12] Jönsson P, Parpia F-A and Froese Fischer C 1996 *Comput. Phys. Commun.* **96** 301
[13] Jönsson P, Andersson M, Sabel H and Brage T 2006 *J. Phys. B: At. Mol. Opt. Phys.* **39** 1813
[14] Froese Fischer C, Brage T and Jönsson P 1997 *Computational Atomic Structure* (Bristol: Institute of Physics Publishing)
[15] McKenzie B-J, Grant I-P and Norrington P-H 1980 *Comput. Phys. Commun.* **21** 233
[16] Isberg B and Litzén U 1985 *Phys. Scr.* **31** 533